

Prediction of Solidification and Phase Transformation of Stainless Steel Weld Metals

Toshihiko Koseki*¹ Hiroshige Inoue*¹
Hiroshi Morimoto*¹ Shigeru Ohkita*¹

Abstract:

Stainless steels are widely used in a variety of corrosive, high-temperature, and cryogenic environments. In the steels' applications, it is important that welding material and welding technique appropriate to each service environment should be developed and supplied in a timely manner. Weldability and weld properties of a stainless steel are greatly affected by the solidification mode of the weld metal. Modeling and other predictive techniques related to solidification and transformation behavior are essential for controlling solidification and subsequent solid-state transformation and for establishing optimum welding techniques. In particular, weld metals for high-performance stainless steels must be higher-alloyed than base metals. This metallurgical overmatching calls for extensive studies over a wide compositional range for the alloy design of the weld metals. The use of a predictive technique for weld solidification and transformation is indispensable for the prompt determination of the optimal weld compositions. In this paper, we summarize the development of a model of weld solidification and transformation by incorporating the thermodynamic calculation of multicomponent alloys, and we discuss the prediction of the solidification and microstructure of austenitic stainless steel weld metals by the use of the model. We also describe the analysis and control of weld solidification and solid-state transformation in various commercial stainless steels and the analysis and prediction of intermetallic precipitates in the as-solidified microstructure of high-alloy weld metals.

1. Introduction

Different types of stainless steels, such as austenitic, ferritic, duplex, and martensitic, are widely used in various corrosive

environments or at very low to high temperatures. Because most of these stainless steels are applied in the form of welded structures, it is important to assure good weldability and weld metal performances required in various environments, in view of the service performance of the total structures. When compared with wrought base metals, weld metals in an as-solidified condition are

*¹ Technical Development Bureau

inferior in performance owing to solute segregation and microstructural heterogeneity. This tendency becomes more significant as the severity of service environments increases, such as highly corrosive environments associated with seawater applications and flue gas desulfurization, and cryogenic or high-temperature environments¹⁾. In weld alloy designs for high-performance stainless steels, it is essential to understand the effect of solidification microstructure on the weld properties and to achieve the optimum solidification and microstructure in the weld metal.

This background has prompted extensive studies on the solidification of stainless steels and their welds. In addition, the solidification modes that determine metallographic features of the final microstructure of welds were clarified²⁻⁵⁾. At the same time, the effects of solidification modes and microstructures on weldability and weld properties were extensively clarified. Fig. 1 schematically illustrates the solidification modes of austenitic stainless steels. The hot cracking tendency of austenitic stainless steels on welds is reduced by the precipitation of delta ferrite (δ -ferrite) during solidification and is lowest with primary δ -ferrite solidification of the FA mode⁹⁾. Cryogenic toughness and high-temperature embrittlement are strongly influenced by the presence, amount, distribution, and morphology of residual δ -ferrite in the solidification microstructure^{6,7)}. The positive or negative microsegregation of solute elements on solidification and the distribution of solute elements in the duplex δ -ferrite/austenite solidification microstructure are mainly responsible for the localized corrosion of welds and promote the precipitation of brittle phases during weld thermal cycles^{1,8,9)}. The effect of solidification on these properties basically applies to weld metals of high alloys, including nickel-based alloys, and weld metals of duplex stainless steels. Prediction and control of weld solidification, and control of the solidification microstructure are extremely important to attain desired weldability and weld properties.

Stainless steels and high alloys, including nickel-based alloys, are fundamentally multicomponent alloys (Fe-Cr-Ni-...) of high solute concentration. Understanding the phase equilibria of multicomponent systems is indispensable when their solidification is analyzed and modeled. In this respect, these high-alloy steels differ greatly from low-alloy steels because, in the latter, solute interaction is relatively insignificant during solidification and the

analysis of solidification behavior can be extrapolated from iron-based binary systems. In high-alloy steels, partition coefficients of solutes between the solid and liquid are not necessarily the same as those derived from binary systems, and the solidification paths are more complicated, including multiphase solidification such as peritectic or eutectic solidification. Phase stabilities on and after solidification are a multivariable function of solute concentrations and cannot be evaluated without information from phase diagrams of multicomponent systems.

Several attempts have been made to analyze the solidification of multicomponent alloys in relation to their phase diagrams, but these attempts have been limited to relatively simple ternary systems. For commercial multicomponent steels, chromium and nickel equivalent equations that include the effect of different solute elements have been empirically derived and applied to either the Fe-Cr-Ni ternary phase diagram or the experimental Schaeffler diagrams¹⁰⁾ to predict solidification behavior and microstructures. As calculation methods for phase diagrams of multicomponent systems by computer (CALPHAD for CALculation of PHase Diagrams) have been extensively developed in recent years, the methods have been applied to the modeling of solidification and other metallurgical phenomena of multicomponent alloys^{11,12)}. The application of phase computation (PHACOMP) using the electron theory is also attempted for the solidification analysis of mainly high alloys^{8,13)}.

Accurate prediction of transformation and precipitation on solidification and post-solidification cooling would be extremely important to control the solidification and microstructure of stainless steel weld metals and to optimize their alloy design. Accurate prediction is also effective in increasing the speed and efficiency of the development of welding technology. As for high-performance stainless steels, weld metals' performance is more inferior to that of base metals if the weld metals match the base metals in chemical composition. For this reason, the welds need to overmatch the base metals metallurgically (or need to be more high-alloyed than the base metals). In the case of high Mo corrosion-resistant stainless steels, for example, severe microsegregation of molybdenum significantly reduces the corrosion resistance of a matching weld metal^{1,9)}. In this case, the weld metal requires a higher molybdenum content than the base metal. To prevent precipitation of brittle phases in an as-solidified condition, compositional optimization need to be studied over a wide compositional range, including nickel-based alloys. Predictive techniques of solidification and transformation would be very effective in reducing the number of necessary experiments and shortening the development period of welding techniques.

Nippon Steel has developed computational models, analyzed the solidification of commercial alloys through experiments and thermodynamic calculations, and derived indexes of microstructural control. All of these efforts are directed toward the prediction and control of solidification and transformation of stainless steels and high-alloy weld metals. These efforts have made it possible to promptly develop welding materials and techniques among various alternatives for weld composition, including overmatching alloy design, appropriate for many steel grades. In the following sections, we describe the models and techniques developed for the prediction and control of weld solidification.

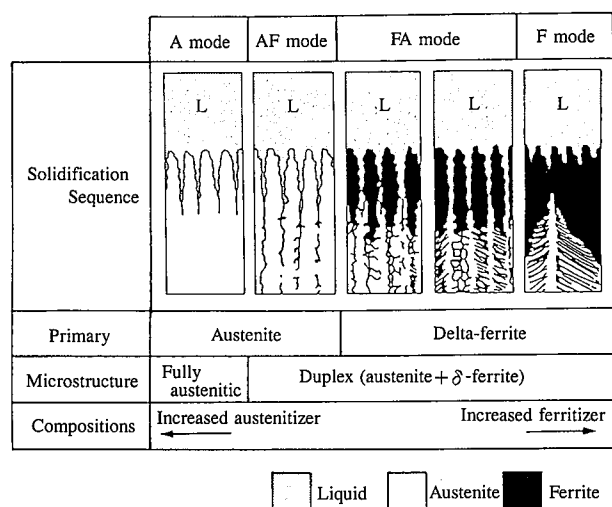


Fig. 1 Schematics of solidification modes of austenitic stainless steels

2. Computational Analysis and Prediction of Solidification

To analyze the solidification of multicomponent alloys, which includes eutectic and peritectic multiphase solidification, a solidification analysis model was combined with Thermo Calc⁽¹⁴⁾, a CALPHAD software⁽¹²⁾. The solidification model evaluated the advance of dendritic solidification by the heat balance and, at the same time, analyzed solute diffusion in the solid phase and the δ/γ solid-state transformation. The shape of solidifying dendrites considered in the model and the computational regime of the model are shown in Fig. 2. The computational flow of the model is shown in Fig. 3. Heat conduction and solid-phase diffusion were assumed in the principal axis direction and radial direction of the dendrites, respectively. Local equilibrium was assumed at

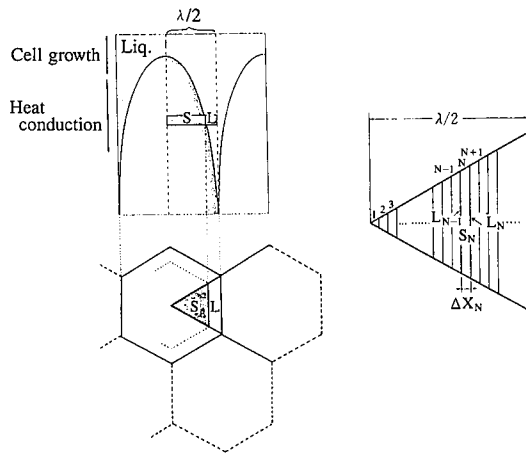


Fig. 2 Longitudinal and transverse sections of a cell considered by solidification analysis mode (a) and computational regime in solidification cell section and difference mesh elements (b)

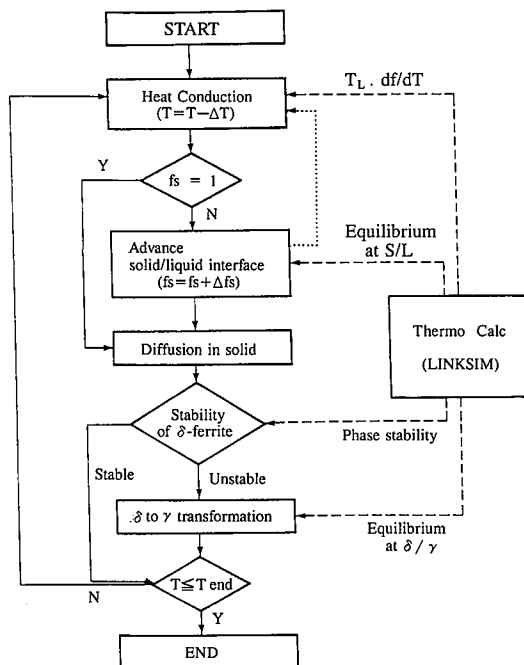


Fig. 3 Flow chart of the solidification analysis model coupled with Thermo Calc

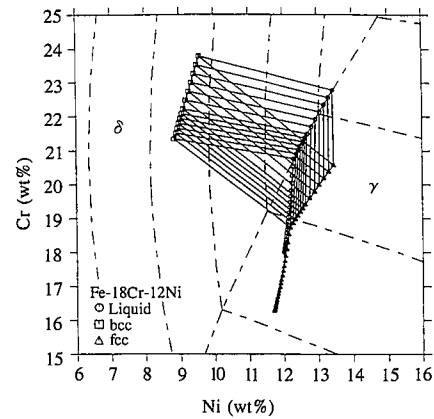


Fig. 4 Analysis results of solidification path of Fe-18Cr-12Ni alloy projected onto the liquidus surface of Fe-Cr-Ni phase diagram

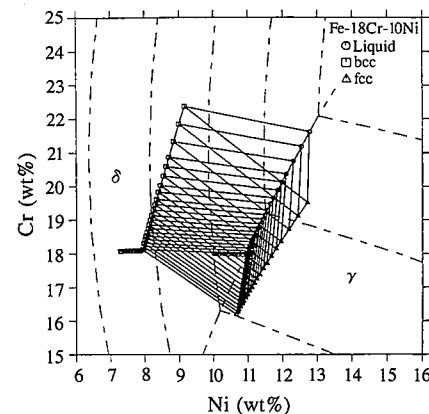


Fig. 5 Analysis results of solidification path of Fe-18Cr-10Ni alloy projected onto the liquidus surface of Fe-Cr-Ni phase diagram

the solid/liquid interface and the δ/γ interface. The phase equilibria of the multicomponent system were calculated by Thermo Calc and introduced into the model as required by the local equilibrium assumption. Microscopic δ/γ transformation in each finite difference element was analyzed by applying the Clyne-Kurz equation⁽¹⁵⁾ to each FDM element, which is independent of macroscopic equilibrium and mass transfer between FDM elements.

The model was applied to Fe-Cr-Ni alloys and compared with experiments⁽¹²⁾. Figs. 4 and 5 show the calculated solidification paths of Fe-18Cr-12Ni and Fe-18Cr-10Ni alloys, respectively projected on the liquidus surface of the ternary phase diagram. The solidification path of the Fe-18Cr-12Ni alloy indicates the transition from primary austenite solidification to the eutectic solidification and simulates the solidification path of the AF mode²⁾ shown in Fig. 1. On the other hand, the solidification path of the Fe-18Cr-10 Ni alloy indicates the transition from δ -ferrite solidification to the eutectic solidification and simulates the solidification path of the FA mode³⁾ shown in Fig. 1. The change of liquid composition to eutectic composition, flexion of the path there, and trace of the eutectic valley are made possible only by the incorporation of the phase diagram computation into the solidification analysis and represent great improvements on conventional solidification analysis models. Fig. 4 shows that the concentration change from the dendrite center to the interdendrite

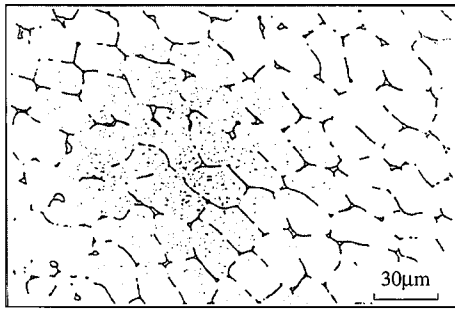


Photo 1 Typical solidification microstructure of Fe-24.6Cr-17.5Ni alloy solidified as primary austenite mode (AF mode)

ic region in the primary austenite solidification is significant for chromium and the solidification path is considerably long for the eutectic fraction of 0.2. Conversely, Fig. 5 shows that the segregation of nickel from the dendrite center to the interdendritic region is predominant in the primary δ -ferrite solidification. These results are in good agreement with the segregation tendency and solute distribution observed in actual stainless steel welds solidified in the AF and FA modes. Photo 1 shows a typical room-temperature microstructure of a weld metal solidified in the AF mode. Solute concentration profiles from dendrite center austenite to interdendritic δ -ferrite measured by scanning transmission electron microscopy (STEM)⁴⁾ are compared with those predicted by the model in Fig. 6. The calculated results agree well with the measurements concerning the chromium enrichment and nickel depletion of interdendritic eutectic δ -ferrite and solute partition between the δ -ferrite and austenite. Good agreements between the calculated and measured values concerning solute distributions are obtained for weld metals solidified in the A and FA modes. Calculated δ -ferrite contents in austenite stainless steel weld metals are compared with measured δ -ferrite contents in Fig. 7. This comparison indicates the ability of the model to predict the amount of retained δ -ferrite relatively well.

Similar verification was performed on commercial stainless steels containing more alloying elements. Fig. 8¹⁶⁾ compares calculated and measured concentration profiles of chromium, nickel, and molybdenum from a dendrite center to an interdendritic region in a type 316 stainless steel weld (Fe-18.5Cr-11.5Ni-2.2Mo) solidified with the FA mode. The calculated values agree well with the measured values concerning chromium and molybdenum enrichment and nickel depletion in the δ -ferrite located at the dendrite center. The model also predicts the content of retained δ -ferrite with relatively high accuracy. The content of retained δ -ferrite and the solute enrichment in the retained δ -ferrite greatly affect the precipitation of brittle phases such as σ phase in weld materials for high-temperature services; their prediction is especially important in this respect.

The validity of the model and the applicability of the model to commercial steels have been confirmed to a considerable degree. To enhance the predictive accuracy of the model, it is necessary to improve the accuracy of thermodynamic data of multicomponent systems and to incorporate such effects as secondary dendrite arms and fluid flow. The model is capable of analyzing the peritectic reaction of not only stainless steels and other high-alloy steels but also low-alloy steels, and the model is expected to be useful for analyzing the solidification of steels on the whole. Attempts are being made to apply the model to the

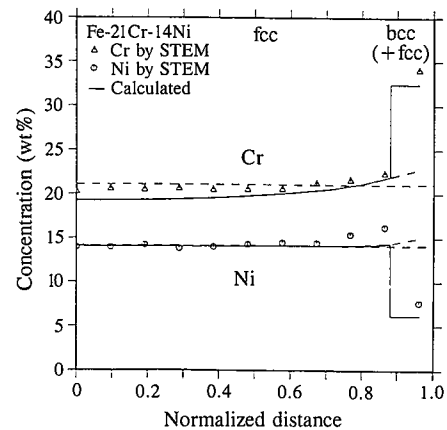


Fig. 6 Comparison of measured and calculated concentration profiles of chromium and nickel in dendrites solidified as primary austenite solidification (AF) mode

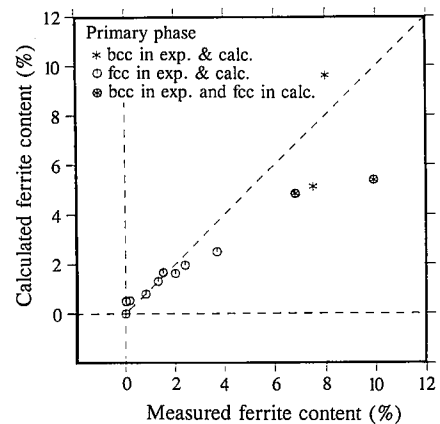


Fig. 7 Comparison of measured and calculated contents of retained δ -ferrite in Fe-Cr-Ni alloy welds

analysis of macrosegregation during steel casting as well as that of microsegregation.

3. Prediction of Solidification and Transformation by Experimentation

In parallel with the development of the solidification model above, studies on the solidification of stainless steels were conducted through experiments and thermodynamic analyses with Thermo Calc. Predictive methods were derived from the studies for the solidification and transformation of the welds and were applied to the development of associated welding technology. The results are described below.

3.1 Effect of nitrogen on solidification of high-nitrogen stainless steel⁶⁾

As discussed, primary phase to solidify has an impact not only on hot cracking resistance of austenitic stainless steel welds but also on the morphology and amount of retained δ -ferrite in the welds and is important in terms of weld properties. In recent years, various high-nitrogen austenitic stainless steels, containing 1,000ppm to 4,000ppm nitrogen, have been developed. Control of the solidification of such high-nitrogen austenitic stainless steel welds calls for quantitative evaluation of the effect of nitrogen on the solidification mode and retained δ -ferrite content of the

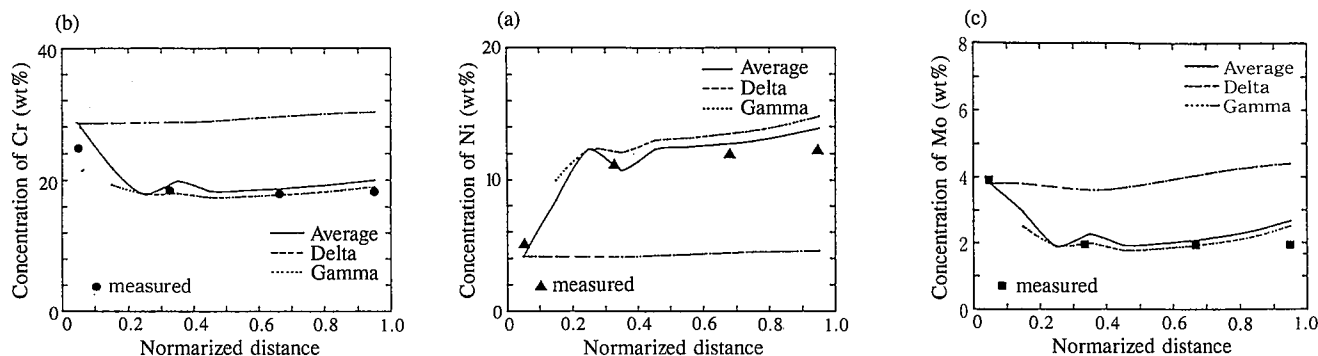


Fig. 8 Comparison of measured and calculated solute distribution in a dendrite of a SUS 316 stainless steel (Fe-18.5Cr-11.5Ni-2.2Mo)

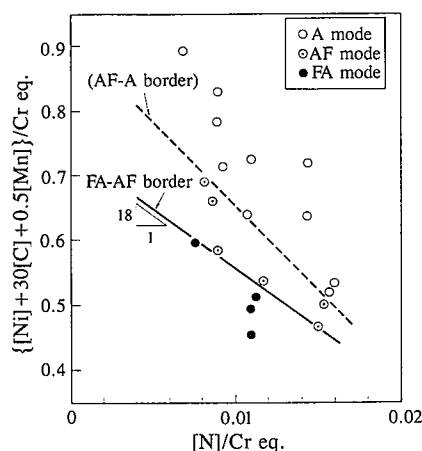


Fig. 9 Effects of nitrogen and other austenite stabilizing elements on solidification mode of high-nitrogen stainless steel weld metals

welds. In Fig. 9⁶⁾, solidification modes of high-nitrogen austenitic stainless steel weld metals are plotted on a coordinate system composed of the nitrogen content and the nickel equivalent from which the nitrogen content is excluded. The dotted line and solid line indicate the boundaries between the A and AF solidification modes and between the AF and FA solidification modes, respectively. The solid line corresponds to the eutectic valley between primary δ -ferrite and primary austenite in multi-component high-nitrogen stainless steel. The slope of the solid line represents the relative strength of nitrogen as an austenitizer compared with nickel; nitrogen's strength is rated as 18 times larger than that of nickel. If the chromium equivalent and modified nickel equivalent are expressed as $\text{Cr} + 1.5\text{Si} + \text{Mo}$ and $\text{Ni} + 30\text{C} + 0.5\text{Mn} + 18\text{N}$, respectively, to describe the solidification of high-nitrogen stainless steel weld metals, the AF-FA mode boundary is located around the chromium/nickel equivalent ratio of 1.36; the primary δ -ferrite FA solidification mode is expected to dominate when the ratio is above 1.36, and the primary austenite solidification mode is expected to dominate when the ratio is under 1.36. The solidification mode of high-nitrogen stainless steel weld metals therefore can be controlled. It was made clear that the content of retained δ -ferrite in the room-temperature microstructure can be predicted by the DeLong nickel equivalent¹⁷⁾, where the nitrogen coefficient was 30. It was demonstrated that nitrogen differs in its strength as an austenitizer relative to nickel when the solidification mode is to be described

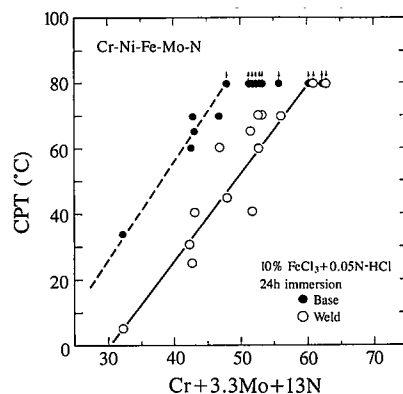


Fig. 10 Relationship between critical pitting temperature (CPT) and pitting index ($\text{Cr} + 3.3\text{Mo} + 13\text{N}$) of Cr-Ni-Fe-Mo-N alloy base metals and weld metals in 10% ferric chloride solution

and when the δ -ferrite content in the final microstructure is to be predicted. This situation is also suggested by a phase diagram study with Thermo Calc and is supported by the kinetic viewpoint; the diffusivity of nitrogen is relatively fast in the solid phase compared with that of other elements. The nitrogen coefficient of 18 in the nickel equivalent derived from Fig. 9 is extremely close to the value suggested by the comparison of the Fe-Cr-Ni and Fe-Cr-Ni-N phase diagrams.

This concept of controlling the solidification mode and microstructure of high-nitrogen stainless steel weld metals was applied to welding techniques for high-strength high-nitrogen stainless steel for cryogenic services⁷⁾ and nitrogen-bearing stainless steels for high corrosion resistance.

3.2 Microstructural control of high-corrosion resistance high molybdenum stainless steel⁸⁾

Problems with the welding of molybdenum-bearing stainless steels are extensive microsegregation of molybdenum in the solidification microstructure and large loss of corrosion resistance in the negative segregation zone of the dendrite center. Fig. 10⁹⁾ compares the corrosion resistance of base metals and as-solidified weld metals. The vertical axis indicates the critical pitting temperature (CPT) in a chloride containing environment, and the horizontal axis indicates the pitting index ($= \text{Cr} + 3.3\text{Mo} + 13\text{N}$). When the weld metal is of the same composition (i.e., pitting index) as the base metal, the weld metal's corrosion resistance is extremely low by negative segregation of the solutes in the solidification microstructure, compared with the base metal.

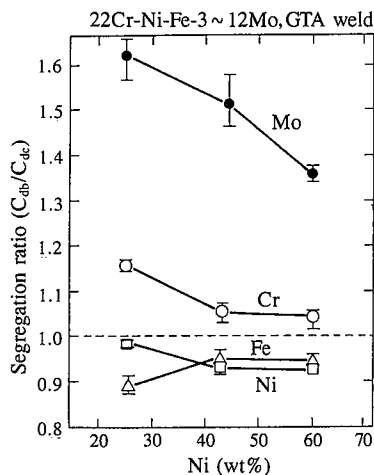


Fig. 11 Effect of nickel on microsegregation ratio (interdendritic/dendrite center concentration) in Cr-Ni-Fe-Mo alloy weld metals

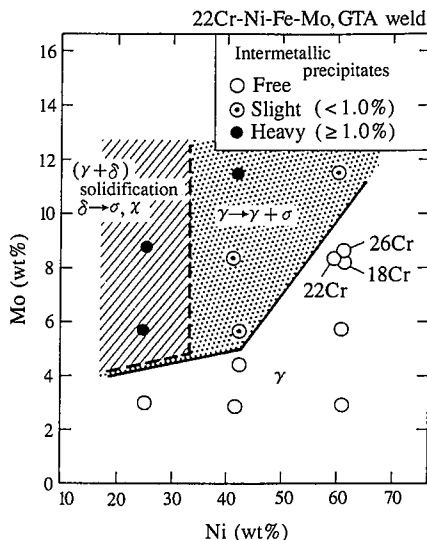


Fig. 12 Effects of nickel and molybdenum on as-solidified microstructure of Cr-Ni-Fe-Mo alloy weld metals

To ensure the desired corrosion resistance of weld metals in chloride containing environments, it is necessary to increase the molybdenum content of the weld metal over that of the base metal and to optimize the microstructure of the weld metal.

Fig. 11⁸⁾ shows the effect of nickel on microsegregation of major elements in welds. The segregation tendency of chromium and molybdenum, which affects corrosion resistance, decreases as nickel content increases. Fig. 12⁸⁾ shows the effects of nickel and molybdenum on the as-solidified microstructure of Cr-Ni-Fe-Mo alloy weld metals. Increasing molybdenum content in iron-based alloys enhances the precipitation of brittle phases such as σ phase. In such alloy systems that precipitate δ -ferrite on solidification, the precipitation of brittle phases from δ -ferrite is significant. A shift from iron base to nickel base reduces the precipitation of brittle phases even with increasing molybdenum content. It was also found that the compositional region where no brittle phases precipitate in Fig. 12 can be expanded to a higher molybdenum range by adding nitrogen.

The effects of nickel and nitrogen on the improvement in solute segregation and reduction in precipitation tendency are well correlated with equilibrium partition coefficients and phase stability calculated by Thermo Calc. It is therefore concluded that such behaviors as solute partitioning at the solid/liquid interface and precipitation in as-solidified structures are governed by equilibrium driving force and local phase stability even in non-equilibrium weld solidification.

The weld metal for high corrosion resistance must have sufficient nickel and molybdenum contents to achieve the optimum microstructure with decreased segregation and precipitation. Nitrogen addition is effective in ensuring the matching of nickel-based welds with the iron-based base metal and in improving corrosion resistance and microstructural integrity in diluted portions. These findings are applied to the welding of high-molybdenum stainless steel with high corrosion resistance for seawater desalination plants and similar applications⁹⁾.

3.3 Microstructural control in duplex stainless steel weld metal^{18,19)}

Duplex stainless steels contain molybdenum and nitrogen, feature a good strength and corrosion resistance, and are widely used in many applications. The fine δ/γ duplex microstructure of the base metal is accomplished by hot rolling and heat treatment in the two-phase region of ferrite and austenite. Welding technology issues to be investigated are how to ensure the desired δ/γ balance in the as-solidified weld metal and how to make up for the microstructural difference between the weld metal and the base metal.

A duplex stainless steel weld metal consists of δ -ferrite, and its duplex microstructure is brought about through δ/γ transformation after solidification. The microstructure of the weld metal consists of coarse δ -ferrite grains with Widmanstätten austenite developed from the δ -ferrite grain boundaries. When the weld metal is of the same composition as the base metal, it is enriched in δ -ferrite and, at the same time, many fine nitrides and carbides precipitate within coarse δ -ferrite grains. Studies of weld solidification and transformation revealed the formation of austenite in the weld metal shows the para-equilibrium behavior as controlled by the diffusion of nitrogen. Therefore, increasing the nitrogen content modifies the δ/γ balance of the weld comparable to that of the base metal, and the formation of nitrides within δ -ferrite grains can be suppressed by a fully developed Widmanstätten austenite. The para-equilibrium between δ -ferrite and austenite was examined on the Fe-Cr-Ni-Mo-N phase diagram by Thermo Calc, as shown in Fig. 13¹⁹⁾. These microstructural studies explain the differences as to δ/γ solute distribution and pitting behavior between the base metal and weld metal and emphasize the importance of increasing the nitrogen content and ensuring the phase balance in the weld metal (see Fig. 14¹⁸⁾).

3.4 Prediction of precipitation of intermetallic compounds in high-alloy weld metal

As stainless steels are increased in alloy content for higher corrosion and heat resistance, inhibiting the precipitation of intermetallic compounds in the as-solidified weld metal becomes a critical issue. Chromium, molybdenum, silicon, and niobium are increased to improve corrosion resistance, oxidation resistance, and elevated-temperature strength. However, these alloying elements have a strong tendency to segregate on solidification and are likely to precipitate harmful brittle phases, such as σ , χ ,

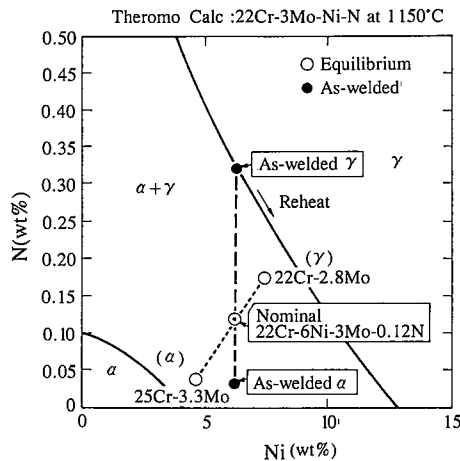


Fig. 13 Comparison of solute partitions in duplex stainless steel and its weld metal

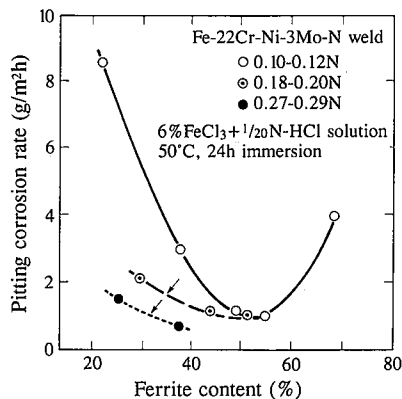


Fig. 14 Effects of ferrite and nitrogen contents on pitting corrosion resistance of duplex stainless steel welds

and Laves phases.

Cieslak et al.¹³⁾ tried to explain the precipitation of σ phase and other topologically close-packed phases in weld metals of nickel-based Hastelloy alloys by applying the phase stability theory (Md-PHACOMP) that Morinaga et al.²⁰⁾ proposed from the electron theory. From the above-mentioned fundamental research into the solidification of weld metals of stainless steels and high-alloy steels, the present authors have demonstrated that local equilibrium still holds for solute partitioning and phase stability on solidification. Based on these findings, they expanded the attempt of Cieslak et al. to the weld metals of stainless steels and high-alloy steels, including iron-base alloys. The Md value that accounts for the phase stability of austenitic multicomponent alloys is calculated in the microsegregation field of welds where the Md value is the sum of the product of the solute concentration and d-electron energy. A typical change in the Md value from a dendrite center to an interdendritic region was compared with the tendency of the precipitation of TCP phases in an as-solidified condition. Fig. 15⁸⁾ shows the relationship between the interdendritic Md value and the fraction of TCP phase precipitates. It was found that when the interdendritic Md value exceeds a critical level of about 0.92, the interdendritic precipitation of TCP phases occurs even in iron-based alloys. Note that this tendency is smaller for nitrogen-bearing alloys. If the

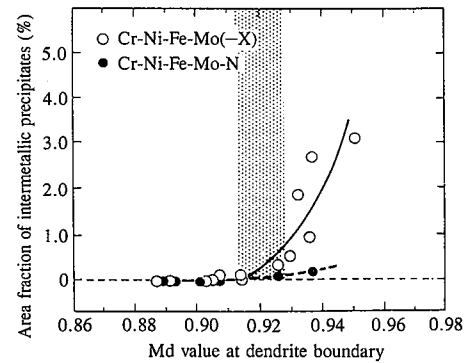


Fig. 15 Relationship between intermetallic compound precipitates and Md values interdendritic regions in as-solidified microstructure of Cr-Ni-Fe-Mo alloy weld metals

microsegregation of a weld metal is predictable a priori, the alloy design of a precipitation-free weld metal would be possible. In that sense, the above-mentioned solidification model or solidification research gains in usefulness.

4. Conclusions

Prediction and control of weld solidification and transformation during welding of stainless steels are extremely important to obtain necessary properties of welds and achieve desired service performances of welded structures. As steels increase in performance and alloy contents, it becomes all the more important to control the solidification and transformation of the weld metal through metallurgical approaches.

The metallurgical approaches worked on by the authors are described by introducing the development of a model to analyze the solidification of multicomponent alloys and by referring to the application of prediction and control techniques to commercial alloys. The solidification and transformation predictive techniques are demonstrated to be effective in the efficient development of welding techniques for various high-performance stainless steels. The diversification of welding processes emphasizes the importance of studying the feasibility of controlling the microstructure of the weld metal from the process standpoints. Basic studies have suggested the feasibility of controlling the microstructure of the weld metal, including metastable phase formation, by undercooling or rapid quenching of the molten steel^{21,22)}. Coupled with the metallurgical approaches discussed above, the microstructural control will have to be studied further as a means for enhancing the service performance of welds and for developing various solidification processes, including high-density energy beam welding.

References

- 1) Garner, A.: Mater. Perform. 21 (8), 321 (1982)
- 2) Takalo, T., Suutala, N., Moisio, T.: Metall. Trans. A. 10A (8), 1173 (1979)
- 3) Suutala, N., Takalo, T., Moisio, T.: Metall. Trans. A. 11A (5), 717 (1980)
- 4) Brooks, J.A., Williams, J.C., Thompson, A.W.: Metall. Trans. A. 14A (1), 23 (1983)
- 5) Brooks, J.A., Thompson, A.W., Williams, J.C.: Weld. J. 63 (3), 71s (1984)
- 6) Ogawa, T., Koseki, T.: Weld. J. 67 (1), 8s (1988)
- 7) Ogawa, T., Koseki, T., Ohkita, S., Nakajima, H.: Weld. J. 69 (6), 205s (1990)
- 8) Koseki, T., Ogawa, T.: Welding International. 6 (7), 516 (1992)

- 9) Ogawa, T., Koseki, T.: Quarterly Journal of Japan Welding Society. 9 (1), 154 (1990)
- 10) Schaeffler, A.L.: Weld. J. 26 (10), 601s (1947)
- 11) Chen, S.W., Chuang, Y.Y., Chang, Y.A., Chu, M.G.: Metall. Trans. A. 22A (12), 2837 (1991)
- 12) Koseki, T., Matsumiya, T., Yamada, W., Ogawa, T.: Metall. Trans. A. 25A (6), 1309 (1994)
- 13) Cieslak, M.J., Knorovsky, G.A., Headley, T.J., Roming, A.D.Jr.: Metall. Trans. A. 17A (12), 2107 (1986)
- 14) Sundman, B., Jansson, B., Andersson, J.O.: CALPHAD. 9, 153 (1985)
- 15) Clyne, T.W., Kurz, W.: Metall. Trans. A. 12A, 965 (1981)
- 16) Ohkita, S., Morimoto, H., Inoue, H., Tanaka, T.: Welding Metallurgy Committee Document, WM-1501-93. 1993
- 17) Long, C.T., DeLong, W.T.: Weld. J. 52 (6), 281s (1973)
- 18) Ogawa, T., Koseki, T.: Weld. J. 68 (5), 182s (1989)
- 19) Ogawa, T., Koseki, T., Inoue, H.: Weldability of Materials. 1990, Materials Park, OH, ASM, p.135
- 20) Morinaga, M., Yukawa, N., Adachi, H.: J. Phy. Soc. Jpn. 53 (2), 653 (1984)
- 21) Inoue, H., Tanaka, T.: Pre-Prints of National Meeting of JWS, 54, 1994, p.236
- 22) Flemings, M.C., Koseki, T.: Proc. Turkdogan Sympo. 1994, Pittsburgh, PA, Iron and Steel Soc. p.207